

SUPPLEMENTARY INFORMATION

Predicting collapse of complex ecological systems: Quantifying the Stability-Complexity Continuum

Journal of the Royal Society Interface

April 27, 2020

Susanne Pettersson^{1*}, Van M. Savage², Martin Nilsson Jacobi¹

Contents

1	Initial species biodiversity or species-pool	2
2	Extinctions when decreasing complexity	2
3	Correlations in the reduced interaction matrices in the Extinction Continuum	4
4	First extinction event	6
4.1	When $r_i = K_i = 1$	6
4.2	The general case of intrinsic growth rates and carrying capacities r and K	7
5	Collapse boundary and persistence	8
6	Estimating initial biodiversity N_{pred}	9
7	The extinction Continuum persists	10
8	The case of large distribution mean μ	16

¹Department of Space, Earth and Environment, Chalmers University of Technology, Maskingränd 2, 412 58 Gothenburg, Sweden.

²Department of Ecology and Evolutionary Biology, Department of Biomathematics, UCLA, Los Angeles, CA, 90095, USA.

1 Initial species biodiversity or species-pool

In our analysis we treat species abundances equal to zero as "complete" extinctions and not only as local phenomena. This is in contrast to other studies which treat the initial biodiversity rather as a species-pool (species present in a region consisting of smaller local communities). In the species-pool interpretation if a species goes extinct in a local community it is not lost and it can still re-invade the local community at a later point in time [1, 2]. Specifically in [1] they found different phases of local community behaviour/turn-over when increasing the mean and variance of interaction strengths. In general increasing turn-over for increasing variance and mean of interaction strength.

The full Jacobian of the system is

$$J_{ij} = \delta_{ij} \left(r_i - 2 \frac{r_i}{K_i} x_i + \sigma \sum_{k=1; k \neq i}^N A_{ik} x_k \right) + \sigma x_i A_{ij}, \quad (1)$$

where r_i and K_i are intrinsic growth rates and carrying capacities respectively, A the interaction matrix with zero diagonal ($A_{ii} = 0$), x_i species abundances, σ the standard deviation of interaction strengths, and δ the Kronecker delta (equal to one when $i = j$ and zero otherwise). A reduced Jacobian J^* for only viable (non-extinct) species, with fixed-point solutions

$$x_i^* = K_i^* / r_i^* \left(r_i^* + \sigma \sum_{k=1; k \neq i}^n A_{ik}^* x_k^* \right), \quad (2)$$

is given by

$$J_{ij}^* = \sigma x_i^* A_{ij}^* - \delta_{ij} \left(\frac{r_i^*}{K_i^*} x_i^* \right) \quad (3)$$

or

$$J^* = X^* (\sigma A^* - D^*),$$

where X^* and D^* in the linear algebra formulation are diagonal matrices with x_i^* and r_i^*/K_i^* on the diagonal respectively. The superscript asterisks indicate the inclusion of only non-extinct viable species. This is the community matrix (Jacobian at a fixed point) which we use in our stability analysis.

At a fixed-point including extinct species the Jacobian for an extinct species i would be

$$J_{ij}^{x_i^*=0} = \delta_{ij} \left(r_i + \sigma \sum_{k=1; k \neq i}^N A_{ik} x_k^* \right). \quad (4)$$

Since this is a diagonal matrix it shows the eigenvalues for the extinct species. For small standard deviation of interaction strengths σ , the eigenvalues are generally negative, hence stable. For larger σ this is not generally the case indicating that the extinct species could re-invade, were they not completely extinct. Thus in the latter part of the Extinction Continuum there can be multiple stable fixed-points in accordance with [2, 3] with different combinations of viable species from a species-pool including "already" extinct ones. Although their basins of attraction differ in size. With no re-invasion on the other hand, larger σ hence less structurally stable systems means a risk of substantial biodiversity reduction if system parameters change (such as r_i or σ), corresponding to the larger turn-over (switching of stable fixed-points) for larger σ found in [1]. The difference then in the two interpretations, complete or local extinctions, is that if system parameters change the structural instability lead to either decreased biodiversity (complete) or turn-over while sustaining biodiversity (local).

2 Extinctions when decreasing complexity

One interesting and perhaps counter intuitive result is that extinctions can occur in the Extinction Continuum as a response to decreasing the standard deviation of interaction strength σ , corresponding to

decreasing complexity. We tested this for systems with random interaction matrices but with intrinsic growth rates r_i specifically chosen to make them resilient and feasible at the complexity boundary introduced by May $\frac{1}{\sqrt{cN}}$. This was done both by brute force sifting through vectors \mathbf{r} with non-negative r_i drawn from truncated Normal and Uniform distributions centred at 1, or allowing for negative r_i , by $\mathbf{r} = (I - \sigma A)\mathbf{x}_{rand}$, with uniformly distributed $x_{i,rand} > 0$. Indeed, we found systems can exhibit species extinctions when σ decreases. This can also occur for our dynamically reduced systems A^* with biodiversity n as seen in Fig. 1.

One interpretation of this response is that for systems to be resilient at levels of complexity high enough to reside in the EC, correlations or interaction patterns have to be in place to accommodate stability. For instance, one species might depend crucially on different species at different levels of complexity, increasing its fragility at these levels if any of the other species go extinct. Thus, correlations seem to be stabilising at specific levels of complexity rather than stabilising for all below the collapse boundary. This makes them sensitive not only to an increase in complexity but also to a decrease, though less so.

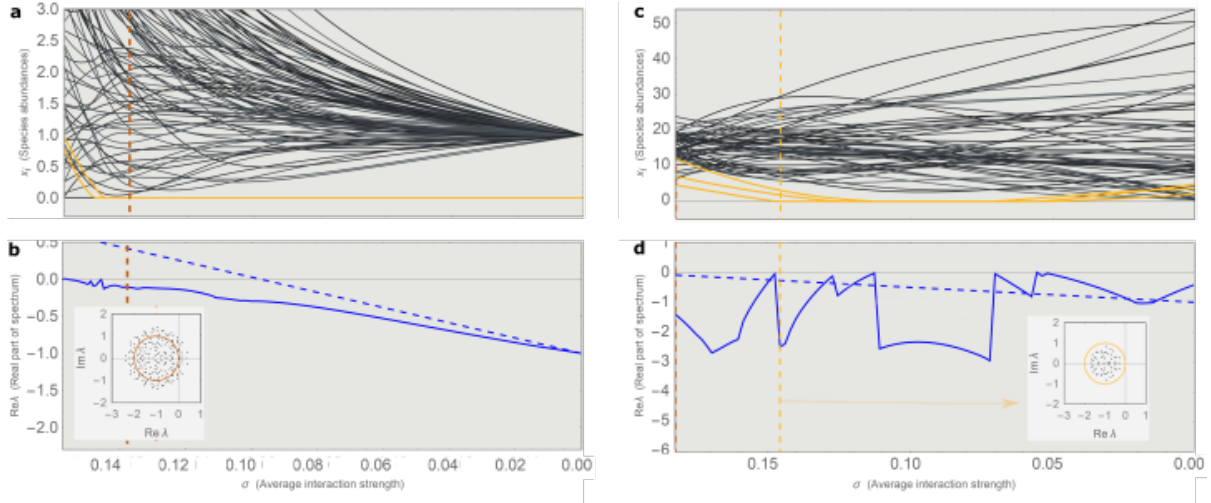


Figure 1 | Species extinctions for decreasing σ . (a,b) An example simulation of a dynamically reduced system with $n = 103$, $c = 0.5$, $K_i = r_i = 1$, and Normally distributed interaction strengths $\text{Normal}(0, 1)$, when decreasing σ . We start the simulation with σ equal to the systems collapse value σ_c when run with increasing σ from zero. The simulation run when increasing σ had initial biodiversity $N = 200$ and was reduced to a viable community of $n = 103$ non-extinct species, which is the starting amount in (a,b). Figure (a) shows that species can go extinct (highlighted in yellow) even when decreasing the interaction strength standard deviation. The leading eigenvalue of the system is shown in (b) (blue line) with the leading eigenvalue of May's model (blue dashed line) and the instability prediction of May's model indicated by the brown dashed line. The inset shows the spectrum of May's model at the instability prediction (for $n = 103$) and maximum stability radius (brown circle), note that the extinctions have changed the stability of the system and the spectrum is no longer contained inside the stability radius. (c,d) These plots show a system with $N = 60$, $c = 0.5$ and Normal distribution $\text{Normal}(0, 1)$ of interaction strengths, where the r_i were chosen such that the system is feasible at the complexity limit introduced by May. Panel (c) Shows a run when decreasing σ from May's limit. The species going extinct are highlighted in yellow and the first extinction when decreasing σ is marked by the yellow dashed line. Panel (d) Shows the leading eigenvalue of the system (blue line) and for May's model (blue dashed line). Both are negative the entire range of interaction strengths, but the actual system can only keep stability by extinctions and resurrections (when the leading eigenvalue is seen to hit zero). The inset shows the spectrum of May's model at the first extinction of the actual model (maximum stability radius in yellow), without any sign of instability or impending extinction.

3 Correlations in the reduced interaction matrices in the Extinction Continuum

Systems with randomly generated interactions that have parameter values N , c and σ placing them in the Extinction Continuum must be dynamically pruned through extinctions (or chosen by some other means) in order to be resilient. This pruning (or choice) makes them no longer random. The simplest argument for this is the statistical result of first extinction boundary for random systems. Since random systems with N , c (c remains constant in the Extinction Continuum see Fig. 2) cannot keep all N species beyond σ_f , some non-random feature must come into play. Two observed changes of dynamically pruned systems is the increase of the interaction strength mean as shown in Fig. 3 and the correlations between (A_{ij}^*, A_{ik}^*) and (A_{ji}^*, A_{ki}^*) noted by [4] for mixed interactions shown in Fig. 4 together with correlations in predator/prey systems.

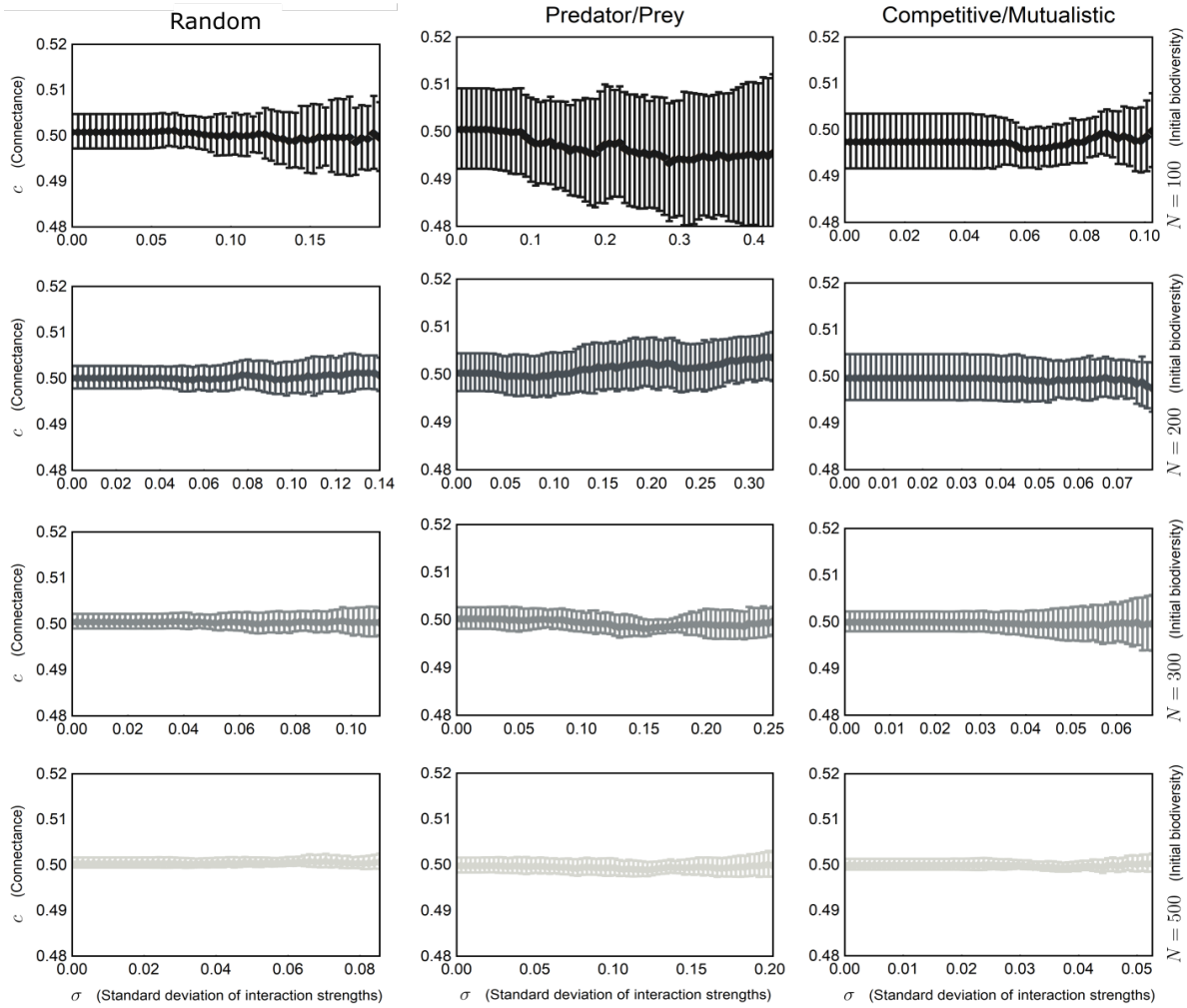


Figure 2 | Connectance of reduced systems. The plot shows the mean connectance and one standard deviation errorbars for the connectance the interaction network of dynamically reduced systems as the standard deviation of the interaction strengths σ is increased. This is shown for systems with *Random*, *Predator/Prey*, and *Competitive/Mutualistic* structures for initial biodiversities $N = 100, 200, 300, 500$. All systems have intrinsic growth rates and carrying capacities $r_i = K_i = 1$. It is clear that the connectance does not change significantly in the Extinction Continuum.

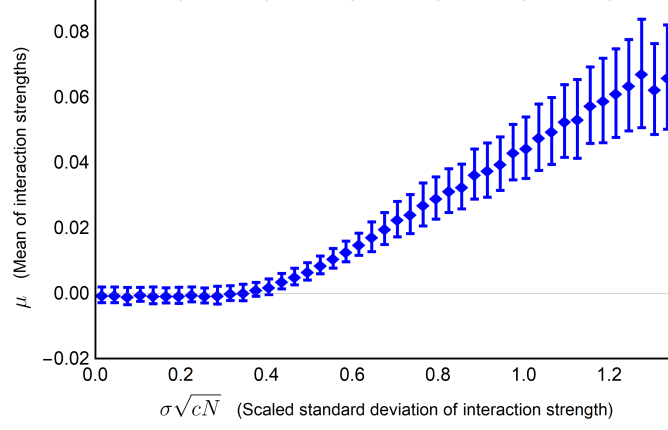


Figure 3 | Increasing mean when increasing standard deviation of interaction strengths. The plot shows means and one standard deviation errorbars for the mean of the interaction strengths μ of dynamically reduced systems as the standard deviation of the interaction strengths σ is increased. The systems initial distribution of interaction strengths $A_{ij} \sim \mathcal{N}(0,1)$, intrinsic growth rates and carrying capacities $r_i = K_i = 1$, connectance $c = 0.5$ and initial biodiversity N ranging between 100 and 500 in steps of 20. It is clear that μ increases in the Extinction Continuum, this is to be expected since species with predominantly negative interactions are expected to go extinct first.

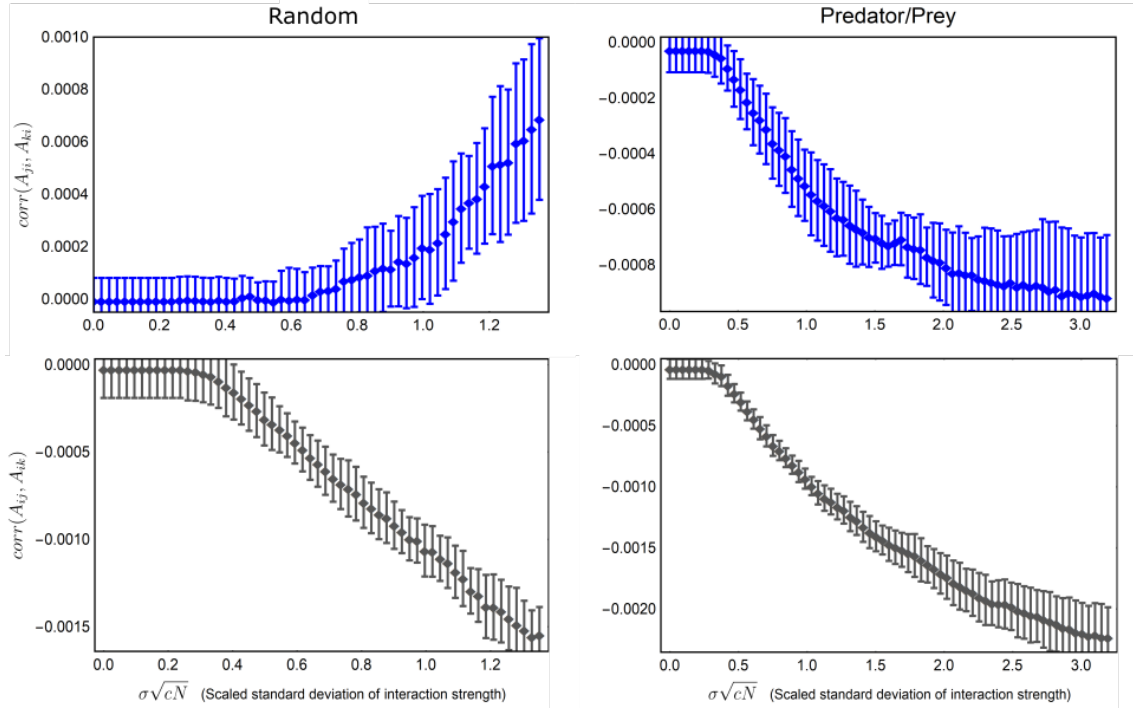


Figure 4 | Increasing correlations when increasing standard deviation of interaction strengths. The figure shows correlation means (10 replicates) with one standard deviation errorbars for systems with $A_{ij} \sim \mathcal{N}(0,1)$ in the *Random* column and for systems with $A_{ij} \sim \mathcal{N}(0,1)$ but in addition $\text{sign}(A_{ij}) = -\text{sign}(A_{ji})$ in the *Predator/Prey* column. All systems have connectance $c = 0.5$, intrinsic growth rates and carrying capacities $r_i = K_i = 1$ and initial biodiversity $N = 500$. The correlation patterns are similar for systems of all sizes although the magnitude of correlations decreases for larger systems. Note the switch from positive to negative correlations in (A_{ji}^*, A_{ki}^*) in predator/prey systems. This might imply that secondary consumers are stabilising, although this is maybe too strong a conclusion because of the lack of trophic hierarchy in these systems.

4 First extinction event

4.1 When $r_i = K_i = 1$

To predict the first extinction boundary we want to find a value of the standard deviation of interaction strength σ_f where it is most likely for a system's first extinction event to occur. Because we are interested in the boundary σ_f of the Strict Stability (SS) phase we can assume feasible fixed points ($x_i^* > 0$ for all $i = 1, 2, \dots, N$ where N is the initial biodiversity). The fixed points written as linear equations for the case $r_i = K_i = 1$ are

$$(I - \sigma A) \mathbf{x}^* = \mathbf{1} \quad (5)$$

where the $\mathbf{1}$ is a vector of ones, I is the identity matrix, \mathbf{x}^* is a vector with fixed point species abundances, and A an $N \times N$ matrix with random interaction strengths from a distribution with mean μ and variance set to one. The more general case for arbitrary r_i and K_i is given below, supplementary information 4.2. To account for competitive and mutualistic systems with mean interaction strength $\mu \neq 0$ we will include these cases in our analysis. To simplify when $\mu \neq 0$ we separate the interaction matrix into $\mathbf{A} = \mathbf{A}_0 + \mu \mathbf{M}$ where the distribution of the entries in \mathbf{A}_0 have mean zero. The diagonal of A is set to zero, the connectance is c and the entries $M_{ij} = 1$ for $A_{ij} \neq 0$. In the case $c = 1$ when all possible interactions are realised, \mathbf{M} is a matrix of ones with zero diagonal. The fixed-point equation can then be written as

$$(\mathbf{I} - \sigma \mathbf{A}_0 - \sigma \mu \mathbf{M}) \mathbf{x}^* = \mathbf{1}. \quad (6)$$

We begin with the case $c = 1$, so $\mathbf{M}\mathbf{x}^*$ can be approximated with the constant vector $x_{TOT}\mathbf{1}$, with $x_{TOT} = \sum_{i=1}^N x_i^*$. The diagonal element is excluded in each sum, but since the variance of the species abundances x_i^* before first extinction is small the approximation is sufficient. The constant vector $x_{TOT}\mathbf{1}$ can be moved to the other side of Eq. 6 and grouped with $\mathbf{1}$. We can then solve for the fixed point abundances

$$\mathbf{x}^* = (\sigma \mu x_{TOT} + 1) (I - \sigma \mathbf{A}_0)^{-1} \mathbf{1}. \quad (7)$$

For the inverse a von Neumann series expansion $((\mathbf{I} - \mathbf{B})^{-1} = \sum_{m=0}^{\infty} \mathbf{B}^m$ for some matrix \mathbf{B} with approximately $|\mathbf{B}| < 1$) to first order gives

$$\mathbf{x}^* \approx (\sigma \mu x_{TOT} + 1) (I + \sigma \mathbf{A}_0) \mathbf{1}. \quad (8)$$

Because the entries of \mathbf{A}_0 are drawn from a random distribution, the species abundances x_i^* can be treated as stochastic variables. We thus get a set of N stochastic variables

$$X_i^* \approx (\sigma \mu x_{TOT} + 1) \left(1 + \sigma \sum_{j=1}^N (A_0)_{ij} \right). \quad (9)$$

Now that we have estimates of species abundances, we can estimate the smallest σ at which there exists a $x_i^* \leq 0$.

Because we assumed $c = 1$, a nonzero μ only adds a scaling factor to X_i^* , hence it will not affect our prediction for when the first species abundance x_i^* becomes zero. Cases when $c < 1$ on the other hand introduce a slight bias. Although we in this case can no longer treat the sum of abundances $\sum_j x_j^*$ in Eq. 8 as a constant x_{TOT} – it is a stochastic variable – it is scaled with the product $\sigma \mu$. When $\sigma \mu$ is small the bias is therefore negligible. Thus, for small $|\mu|$ the scaling factor x_{TOT} for all values of c does not impact our estimate of first extinction.

The distributions of the X_i^* are row sums of the interaction matrix \mathbf{A}_0 . For a normal distribution of the interaction strengths or any distribution so long as the product of initial biodiversity and connectance is large ($cN \gg 1$) enough to invoke the central limit theorem, the sums are normally distributed

$$\begin{aligned} X_i^* &= 1 + \sigma ((A_0)_{i1} + (A_0)_{i2} + \dots (A_0)_{iN}) \\ &\sim \mathcal{N}(\mu_+ = 1, \sigma \sqrt{cN}), \end{aligned} \quad (10)$$

where μ_+ and $\sigma^2 cN$ are the new means and variances for the sums. The extra cN , appearing in the variance is the mean of the Binomial distribution of N trials with success probability equal to the connectance c .

From order statistics we get the distribution for the minimum species abundance ($f_{min}(x)$) in the set of abundances from the distribution function of X_i^* ($f(x)$) and its cumulative distribution function, $F(x)$,

$$f_{min}(x) = N(1 - F(x))^{N-1} f(x) \\ = \frac{N e^{-(x-\mu_+)^2/2\sigma^2 cN}}{\sigma \sqrt{2\pi cN}} \left(\frac{1}{2} - \frac{1}{\sqrt{\pi}} \int_0^{\frac{x-\mu_+}{\sigma \sqrt{2cN}}} e^{-t^2} dt \right)^{N-1}. \quad (11)$$

The first extinction event is then predicted at the σ_f for which the mean of the above distribution is zero. This prediction is in well agreement with simulations as shown in Fig. 2 in the main text.

4.2 The general case of intrinsic growth rates and carrying capacities r and K

We have established that the first extinction event for the case when $r_i = K_i = 1$ occurs at the σ for which we get a mean of zero for the minimum distribution $f_{min}(x)$ of the set of all species abundances

$$f_{min}(x) = N(1 - F(x))^{N-1} f(x). \quad (12)$$

Where the initial biodiversity is N , $f(x)$ and $F(x)$ are the distribution function and the cumulative distribution function of the species fixed point abundances x_i^* ($i = 1, 2, \dots, N$) respectively. For the more general case of r_i and K_i drawn from distributions the row sums of A used to get the species abundances are now sums weighted by r_i and K_i . Thus we need to do more work to capture this extra variability.

The usual version of the GLV which gives the Jacobian in Eq. 1, and which is used in the main text is

$$\frac{dx_i}{dt} = r_i x_i \left(1 - \frac{x_i}{K_i} \right) + \sigma x_i \sum_{j=1}^N A_{ij} x_j. \quad (13)$$

The equations can also be formulated slightly different as

$$\frac{dx_i}{dt} = x_i \left(r_i - \frac{x_i}{K_i} \right) + \sigma x_i \sum_{j=1}^N A_{ij} x_j, \quad (14)$$

where r_i is the intrinsic growth rate only affecting the linear term (and not the intraspecific interaction). On the other hand this formulation changes the carrying capacity when no interspecific interactions are present to $r_i K_i$ instead of K_i . When investigating the GLV we have used both versions, and found them to be qualitatively equal. We show the derivation of the first extinction for r_i and K_i when drawn from distributions for the second version of the GLV as in Eq. 14, although the procedure is the same for both versions and as mentioned, with qualitatively equal results. We begin with the case of $\mu = 0$. The fixed point abundances for the general case of Eq. 14 written as a linear equation are

$$\mathbf{x}^* = (K^{-1} - \sigma A)^{-1} \mathbf{r} \\ = K (I - \sigma A K)^{-1} \mathbf{r}, \quad (15)$$

where K is a diagonal matrix with K_i on the diagonal and \mathbf{r} a vector with intrinsic growth rates. When locating the first extinction event we interpret the fixed point abundances, intrinsic growth rates and carrying capacities as stochastic variables X_i^* , R_i and K_i . Using a von Neumann expansion to first order for the inverse in equation 15 as outlined in Sec. 4.1, we get an equation for the abundances as

$$X_i^* = K_i \left(R_i + \sum_{j=1}^N A_{ij} R_j K_j \right). \quad (16)$$

Here we are assuming a small variance of K_i for the von Neumann expansion to hold. When R_i and K_i are no longer constant but drawn from distributions, X_i^* cannot be approximated by the normal distribution

as before. This is because we add and multiply by stochastic variables R_i and K_i . A product distribution of two stochastic variables Z and Y with distribution functions $f_Z(z)$ and $f_Y(y)$ respectively, has the form

$$f_W(w) = \int_{-\infty}^{\infty} f_Z(z) f_Y(w/z) \frac{1}{|z|} dz. \quad (17)$$

A sum of two random variables Z and Y has the distribution function

$$f_W(w) = \int_{-\infty}^{\infty} f_Y(w - z) f_Z(z) dz. \quad (18)$$

Combining the three distribution $f_R(r)$, $f_K(k)$, and $f_N(y)$, where the first two are for R_i and K_i respectively, and the last is from the sum, $\sum_{j=1}^N A_{ij} K_j R_j$, we get

$$f_X(x) = \int_{-\infty}^{\infty} \left(\int_{-\infty}^{\infty} f_N(z - r) f_R(r) dr \right) f_K(x/z) \frac{1}{|z|} dz, \quad (19)$$

with CDF

$$F_X(x) = \int_{-\infty}^x \left(\int_{-\infty}^{\infty} \left(\int_{-\infty}^{\infty} f_N(z - r) f_R(r) dr \right) f_K(x/z) \frac{1}{|z|} dz \right) dx. \quad (20)$$

These are the more general functional forms to plug into the minimum distribution in Eq. 12. The mean and variance of the normally distributed sum ($\sum_{j=1}^N A_{ij} K_j R_j$), must also be updated since the row entries of A are now weighted by the product of R_i and K_i . The mean and variance of the product of the three stochastic variables, $A_{ij} K_j R_j$, are

$$\begin{aligned} \mu_{AKR} &= \mu \times \mu_K \times \mu_R = 0 \\ \sigma_{AKR}^2 &= \sigma^2(\sigma_K^2 + \mu_K^2)(\sigma_R^2 + \mu_R^2) - \mu_{AKR}^2, \end{aligned} \quad (21)$$

and since we have the density c and the size of the system N , the entire sum is

$$\begin{aligned} \mu_N &= cN \mu_{AKR} = 0 \\ \sigma_N^2 &= cN \sigma_{AKR}^2. \end{aligned} \quad (22)$$

Hence, we get $f_N(y = z - r) \sim N(\mu_N, \sigma_N^2)$ in Eqs. 19 and 20 above. In supplementary Fig. 7 this prediction is shown to be in good agreement with simulations.

For the case of $\mu \neq 0$ we can extract μ from A as done in Eq. 6 and von Neumann expand the inverse in Eq. 15 to get the fixed point abundances as

$$\mathbf{x}^* \approx K (I + \sigma A K) \left(\sigma \mu \sum_{j=1}^N x_j \mathbf{1} + \mathbf{r} \right). \quad (23)$$

Where $\mathbf{1}$ is a constant vector of ones as in Eq. 8. In this form we see that even if $c = 1$ (making the sum $\sigma \mu \sum_{j=1}^N x_j$ constant and equal for every species) nonzero values of μ in the interaction matrix A will add to the mean of R_i and thus affect when the first extinction occurs. This will shift the value of σ of first extinction to smaller values when $\mu < 0$ and larger values when $\mu > 0$. The effect is increased for $c < 1$ when the sum of abundances is a stochastic variable, and as in the case of $r_i = K_i = 1$, the effect is more pronounced for $\mu > 0$ because of larger species abundances in the sum due to the higher degree of mutualistic interactions in A .

5 Collapse boundary and persistence

To locate the collapse boundary σ_c we use a method connected to persistence – the fraction of viable species for a specific choice of parameters. We estimate persistence, p , by the non-trivial fixed point solutions to $\mathbf{x}^* = (D - \sigma A)^{-1} \mathbf{r}$, corresponding to specific values of r_i , K_i (r_i/K_i on the diagonal of the diagonal matrix D), and the other GLV parameters, σ , μ and structure of A . For systems of size N

with values of $\sigma > \sigma_f(N)$ – larger standard deviation of interaction strength than for the predicted first extinction boundary – the non-trivial solution will include negative x_i^* . Although the positive x_i^* are not the fixed-point abundances of a reduced viable system with biodiversity n , the number of positive entries, $n_+(\sigma) = \mathbf{x}^* \mathbf{\Theta}$ (where $\mathbf{\Theta}$ is a vector of Heaviside step functions), can be used for an approximation of the persistence, $p(\sigma) = n_+(\sigma)/N$. In Fig. 3 in the main text we show the statistics of prediction of the persistence obtained from the non-negative abundances compared to the actual persistence for systems of varying sizes ($N = 20 - 1000$).

The reduced system corresponding to the positive abundances and persistence opens up two ways of predicting collapse. First approach, we use the reduced system of positive fixed-point entries and $J^* = \sigma A^* - D^*$ (since the reduced system is feasible), to calculate collapse as the σ where the reduced system loses stability. The second approach is to find the σ at which the number of remaining species $n_+(\sigma)$ (number of positive fixed point entries) would be at the complexity limit introduced by May, meaning σ_c fulfils $\sigma \sqrt{cp_c N} = 1$, where p_c is $p(\sigma_c)$. This works well since May's limit is known to be a good predictor of collapse when assuming feasibility. For both these approaches, statistics were collected for different realisations in simulations, and we use the average as a predictor of collapse.

6 Estimating initial biodiversity N_{pred}

To estimate the size of the initial biodiversity N_{pred} from the measurable quantities of a system in the Extinction Continuum we use a rate of extinction based on the given interaction matrix A^* , for the known biodiversity n . From A^* we get a the number of non-extinct species for increasing values of σ as the positive fixed point solutions to the linear equation

$$\mathbf{x} = \left(\frac{r_i^*}{K_i^*} I^* - \sigma A^* \right)^{-1} \mathbf{r}, \quad (24)$$

thus giving us an average rate of extinction for the community in question. With this rate we extrapolate linearly to the interaction standard deviation of our first extinction prediction for the community σ_f (based on the biodiversity of the community n), as shown in Fig. 5. This gives a prediction for N_{pred} . For systems that are close to collapse the rate obtained in this way tends to diverge. To avoid this we also use an average extinction rate obtained from many runs with systems of all sizes (approximately $rate = -1$), then scaled to fit the specific system size in question $rate \sqrt{cn^3}$. This average rate is used when the predicted specific system rate becomes unrealistically large.

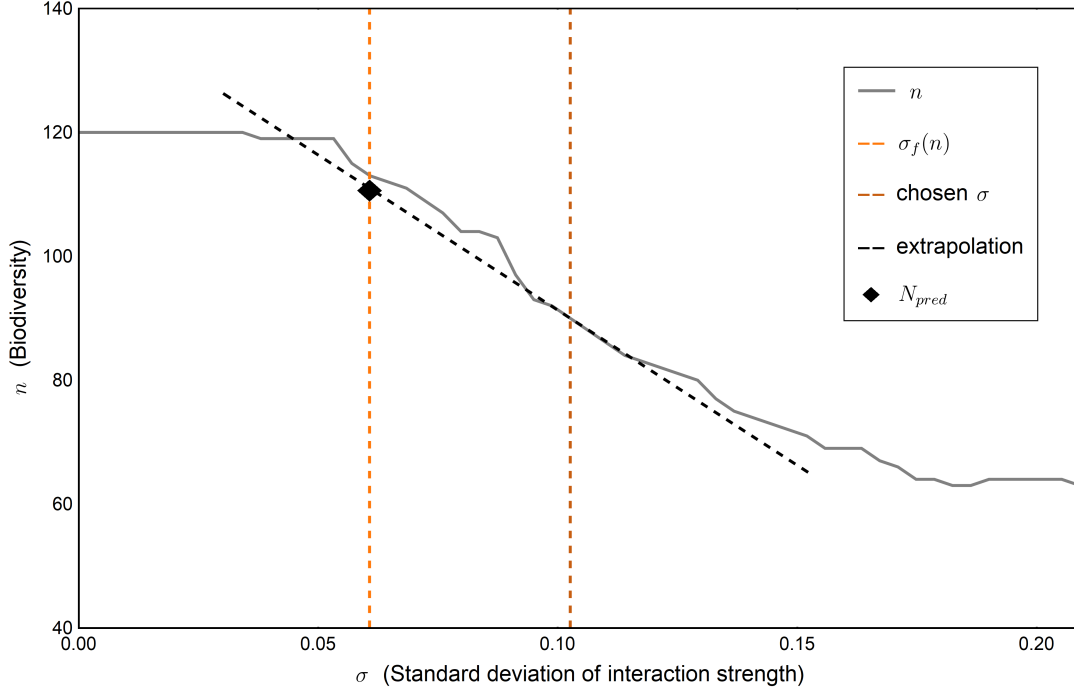


Figure 5 | Finding N_{pred} . The plot shows the extrapolation (black striped line) with the use of an extinction rate obtained from the interaction matrix A^* for a system in the Extinction Continuum with $n = 90$ species and $\sigma = 0.1$. The size of the initial biodiversity for this system is $N = 120$ and the prediction obtained is $N_{pred} = 111$ marked where the striped orange line indicating the first extinction prediction from n and extrapolation line cross. The grey line is the amount of non-extinct species for the simulated system.

7 The extinction Continuum persists

The Extinction Continuum and associated single species extinction stabilising mechanism hold not only for systems with a standard setup of random interactions between species (no imposed structure, for example, predator-prey), interaction strengths sampled from a normal distribution with a mean of zero and variance of one and of specific sizes as shown in Fig. 2 in the main text. In Figs. 6-10 we show that there are no qualitative differences in results even if any of the assumptions on distribution, structure, mean, r_i , and K_i respectively are modified. The figures also show our predictions of the two boundaries surrounding the Extinction Continuum.

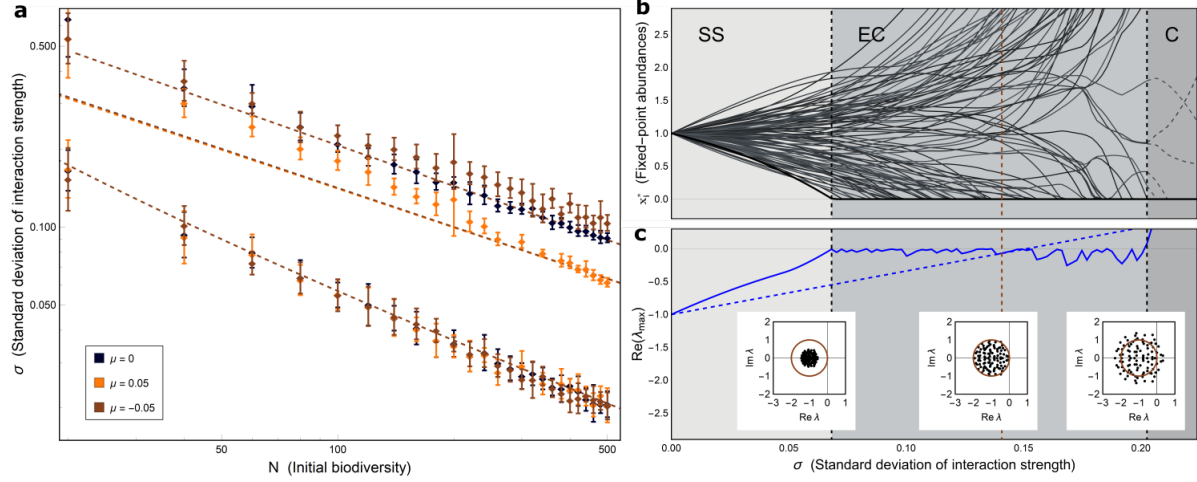


Figure 6 | Increasing interaction variability in complex systems with $\mu \neq 0$. (a) Is a log-log plot showing standard deviation of interaction strength for first extinction, extended May's limit [5] and collapse vs. initial biodiversity N for a random system with Normally distributed interaction strengths with $\mu = 0$ (black) and two systems with $\mu = -0.05$ (brown) and $\mu = 0.05$ (yellow) respectively. The dots are simulated values with one standard deviation errorbars and the striped lines are our theoretical predictions. All systems have intrinsic growth rates and carrying capacities $r_i = k_i = 1$ and connectance $c = 0.5$. (b,c) Show a specific run for a system with $\mu = -0.05$, $c = 0.5$ and $N = 100$. (b) Shows fixed-point species abundances x_i^* for varying σ . The shaded background indicates the three phases Strict Stability (SS), Extinction Continuum (EC) and Collapse (C). The three dashed lines show the two boundaries first extinction and collapse with the limit introduced by May in between. (c) Shows the the leading eigenvalue of the system (blue line) and the leading eigenvalue for the same system when assuming feasibility (not including fixed point species abundances in the Jacobian), blue dotted line. The insets show the spectrum of the Jacobian excluding the species abundances at the two boundaries and May's limit with the circle indicating the stability radius. It is clearly seen that the Extinction Continuum with single species extinctions to uphold community resilience is present also in the case for $\mu \neq 0$.

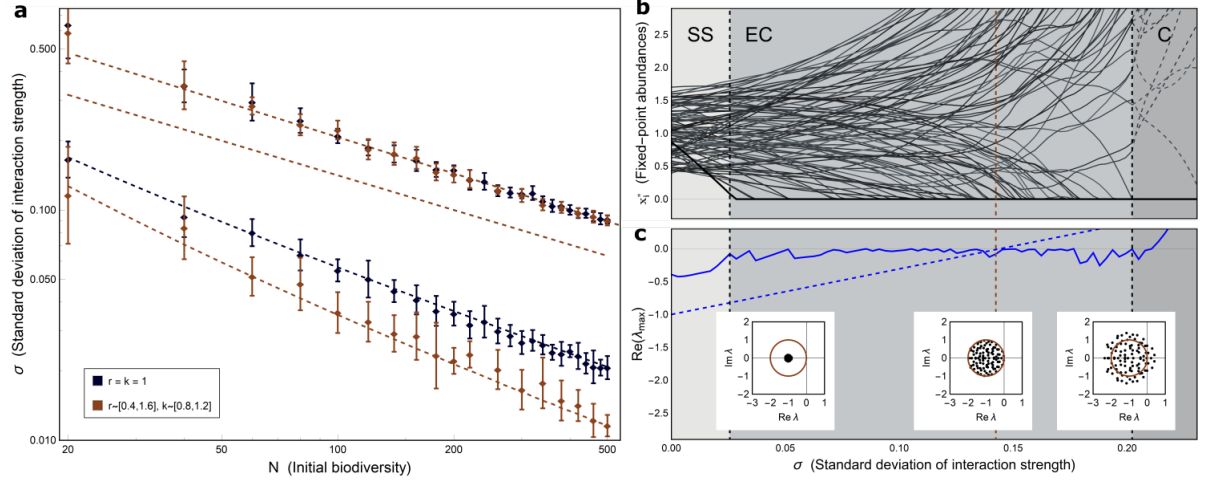


Figure 7 | Increasing interaction variability in complex system for r_i and k_i with non-zero variance. (a) Is a log-log plot showing standard deviation of interaction strength for first extinction, May's limit and collapse vs. initial biodiversity N for a random system with $r_i = k_i = 1$ (black) and a system with r_i and k_i drawn from uniform distributions $\text{Unif}(0.4, 1.6)$ and $\text{Unif}(0.8, 1.2)$ respectively (brown). The dynamics is according to 14. The dots are simulated values with one standard deviation errorbars and the striped lines are our theoretical predictions. Both systems have $\text{Normal}(0, 1)$ for the entries in the interaction matrix and connectance $c = 0.5$. (b,c) Show a specific run for a system with varying r_i and k_i , $c = 0.5$ and $N = 100$. (b) Shows fixed point species abundances x_i^* for varying σ . The shaded background indicates the three phases Strict Stability (SS), Extinction Continuum (EC) and Collapse (C). The three dashed lines show the two boundaries first extinction and collapse with the limit introduced by May in between. (c) Shows the the leading eigenvalue of the system (blue line) and the leading eigenvalue for the same system when assuming feasibility (not including fixed point species abundances in the Jacobian), blue dotted line. The insets show the spectrum of the Jacobian excluding the species abundances at the two boundaries and May's limit with the circle indicating the stability radius. It is clearly seen that the Extinction Continuum is present even in cases when r_i and k_i are drawn from distributions. Although with a large enough variance in r_i the SBS phase will disappear.

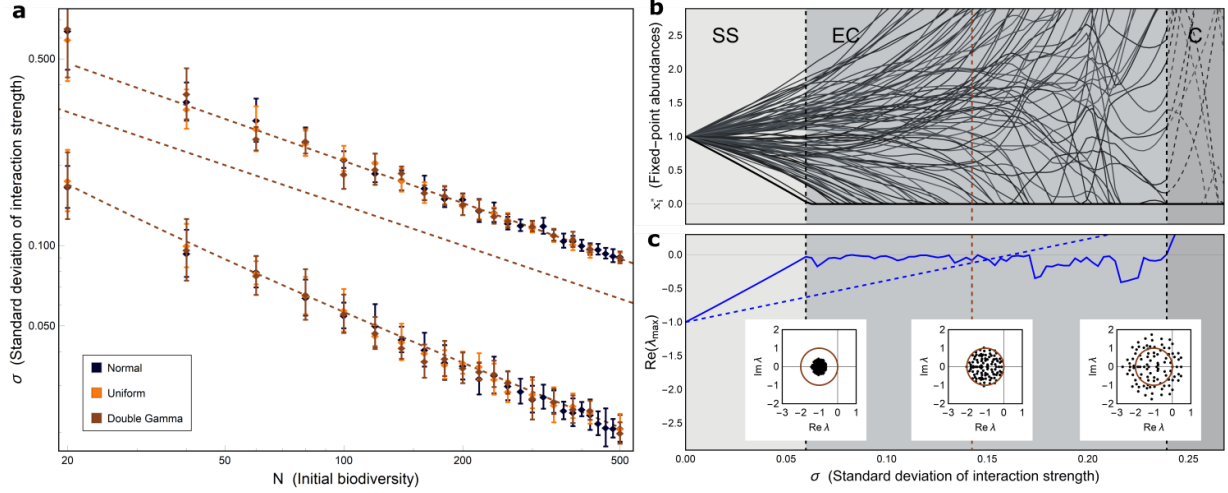


Figure 8 | Increasing interaction variability in complex systems with different interaction strength distributions. (a) Is a log-log plot showing standard deviation of interaction strength for first extinction, May's limit and collapse vs. initial biodiversity N for a random system with interaction strength distribution Normal(0, 1) (black) and two systems with Uniform($-1/\sqrt{3}, 1/\sqrt{3}$) (yellow) and a mirrored Gamma distribution MirrorGamma(0, 1) respectively. The dots are simulated values with one standard deviation errorbars and the striped lines are our theoretical predictions. All systems have intrinsic growth rates and carrying capacities $r_i = k_i = 1$ and connectance $c = 0.5$. (b,c) Show a specific run for a system with MirrorGamma(0, 1) interaction strength distribution, $c = 0.5$ and $N = 100$. (b) Shows fixed point species abundances x_i^* for varying σ . The shaded background indicates the three phases Strict Stability (SS), Extinction Continuum (EC) and Collapse (C). The three dashed lines show the two boundaries first extinction and collapse with the limit introduced by May in between. (c) Shows the the leading eigenvalue of the system (blue line) and the leading eigenvalue for the same system when assuming feasibility (not including fixed point species abundances in the Jacobian), blue dotted line. The insets show the spectrum of the Jacobian excluding the species abundances at the two boundaries and May's limit with the circle indicating the stability radius. It is clearly seen that Extinction Continuum is present also for different interaction strength distributions. It has been previously shown that, as long as the distributions have the same mean and variance they will have equal May limits [5], our boundary predictions show that this also holds for first extinction and the collapse boundary.

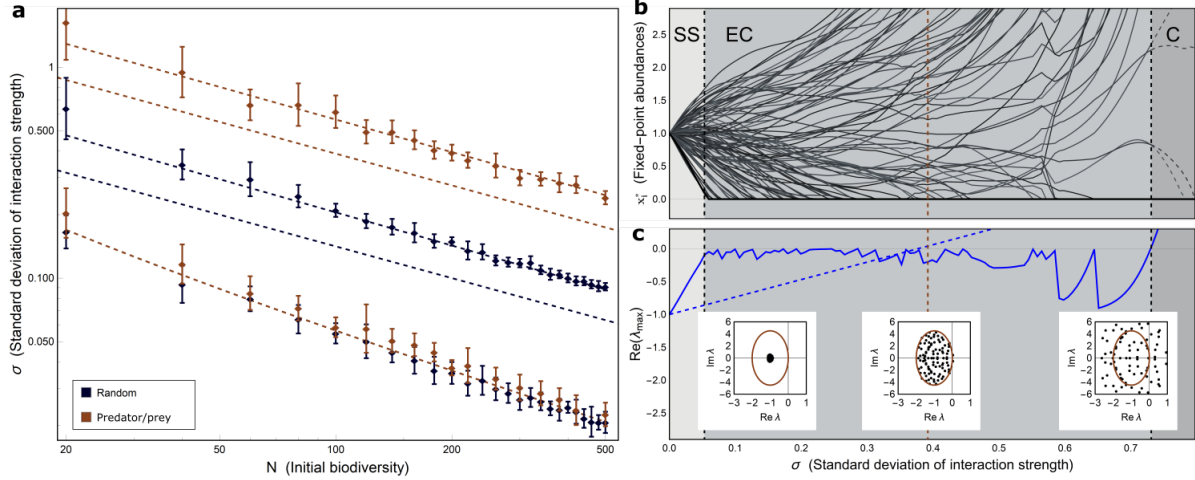


Figure 9 | Increasing interaction variability in a complex system with predator-prey structure. (a) Is a log-log plot showing standard deviation of interaction strength for first extinction, extended May's limit [5] and collapse vs. initial biodiversity N for a random system without any structure in the interaction matrix (black) and a system with predator-prey structure $\text{sign}(a_{ij}) = -\text{sign}(a_{ji})$ (brown). The dots are simulated values with one standard deviation errorbars and the striped lines are our theoretical predictions. All systems have intrinsic growth rates and carrying capacities $r_i = k_i = 1$, Normally distributed interaction strengths $\text{Normal}(0, 1)$ and connectance $c = 0.5$. (b,c) Show a specific run for a system with predator-prey structure and $N = 100$. (b) Shows fixed point species abundances x_i^* for varying interaction variability. The shaded background indicates the three phases Strict Stability (SS), Extinction Continuum (EC) and Collapse (C). The three dashed lines show the two boundaries first extinction and collapse with the limit introduced by May in between. (c) Shows the the leading eigenvalue of the system (blue line) and the leading eigenvalue for the same system when assuming feasibility (not including fixed point species abundances in the Jacobian), blue dotted line. The insets show the spectrum of the Jacobian excluding the species abundances at the two boundaries and May's limit with the oval indicating the stability radius. It is clearly seen that including persistence in the analysis radically changes stability predictions introducing the Extinction Continuum also for systems with predator-prey structure.

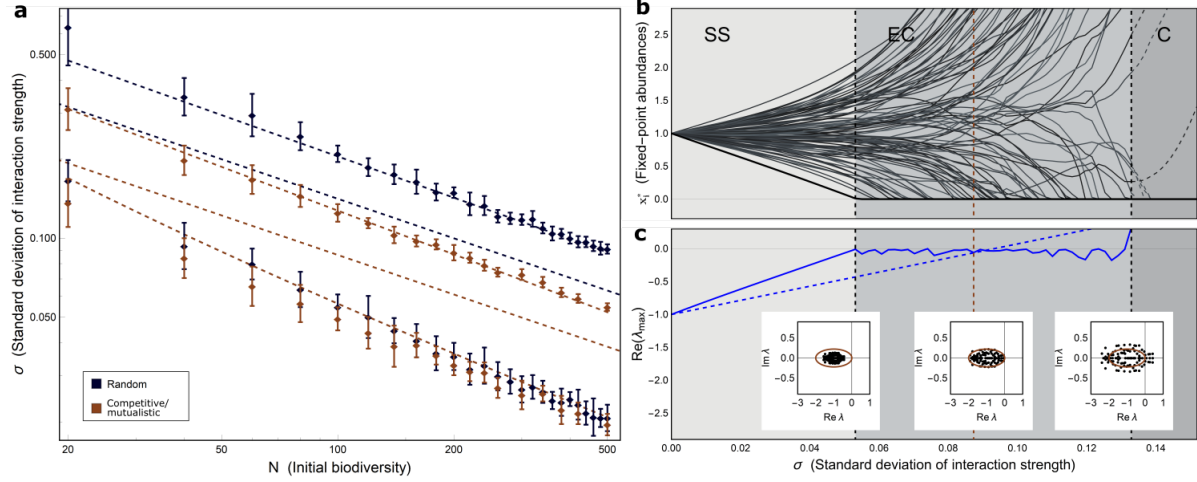


Figure 10 | Increasing interaction variability in a complex system with mutualistic and competitive interactions. (a) Is a log-log plot showing standard deviation of interaction strength for first extinction, extended May's limit [5] and collapse vs. initial biodiversity N for a random system without any structure in the interaction matrix (black) and a system with only mutualistic and competitive interactions $\text{sign}(a_{ij}) = \text{sign}(a_{ji})$ (brown). The dots are simulated values with one standard deviation errorbars and the striped lines are our theoretical predictions. All systems have intrinsic growth rates and carrying capacities $r_i = k_i = 1$, Normally distributed interaction strengths $\text{Normal}(0, 1)$ and connectance $c = 0.5$. (b,c) Show a specific run for a system with predator-prey structure and $N = 100$. (b) Shows fixed-point species abundances x_i^* for varying σ . The shaded background indicates the three phases Strict Stability (SS), Extinction Continuum (EC) and Collapse (C). The three dashed lines show the two boundaries first extinction and collapse with the limit introduced by May in between. (c) Shows the the leading eigenvalue of the system (blue line) and the leading eigenvalue for the same system when assuming feasibility (not including fixed point species abundances in the Jacobian), blue dotted line. The insets show the spectrum of the Jacobian excluding the species abundances at the two boundaries and May's limit with the oval indicating the stability radius. It is clearly seen that including persistence in the analysis changes the stability predictions and introduces the Extinction Continuum also for cases when species interactions are strictly mutualistic or competitive.

8 The case of large distribution mean $|\mu|$

As noted in the main text section 2.2 the γ measure of proximity to collapse is not reliable for a mean of the interaction strengths with significantly larger absolute value than zero. This is because we estimate σ_c (loss of stability) based on when the matrix $\sigma A^* - D^*$ (with D^* a diagonal matrix with r_i/K_i on the diagonal), for a reduced system estimated by the positive entries of the non-trivial solution to equation

$$\mathbf{x}^* = (D^* - \sigma A^*)^{-1} \mathbf{r}^*, \quad (25)$$

loses stability. This is not the actual Jacobian of the reduced system which would be $X^*(\sigma A^* - D^*)$, where X^* is a diagonal matrix with the fixed point abundances of the reduced system on the diagonal. Not including the fixed-point abundances (since they are feasible for the reduced systems and assumed not to alter stability outcome with D-stability arguments [6]) is the approach that May and many after him use to approximate the collapse boundary. This is a more general approach since it does not need the species abundances and therefore not the specification of a system.

Generality on the other hand has its costs, even in addition to not including extinctions. In our boundary predictions we are taking extinctions into account by using the persistence, but there is a difference in magnitude of the fixed-point abundances of the real (simulated) system depending on sign and magnitude of a non-zero μ . These magnitude differences in species abundances acts either to destabilise or stabilise the Jacobian which is not accounted for since we approximate stability without abundances.

For systems with $\mu > 0$ there is a prevalence of mutualistic interactions making the fixed point abundances larger and thus destabilising the Jacobian for smaller values of σ . Equally when $\mu < 0$ there will be more competitive interactions keeping the abundances in check which stabilises the Jacobian leading to a collapse boundary at larger σ . It is an interesting observation that simulated systems with larger non-zero $|\mu|$ do not, as for the $\mu \approx 0$ case, agree with the theoretical predictions for larger $|\mu|$ [5]. For these reduced systems collapse occurs at larger/smaller values of σ due to the inclusion of species abundances.

An approach to handling the influence of species abundances could be to use either the positive fixed-point entries or fixed point solutions to the reduced system as an approximation of the actual species abundances. This however did not help to predict the collapse for systems with large $|\mu|$.

References

1. Kessler, D. A. & Shnerb, N. M. Generalized model of island biodiversity. *Physical Review E* **91**, 042705 (2015).
2. Bunin, G. Ecological communities with Lotka-Volterra dynamics. *Physical Review E* **95**, 042414 (2017).
3. Biroli, G., Bunin, G. & Cammarota, C. Marginally stable equilibria in critical ecosystems. *New Journal of Physics*. ISSN: 1367-2630 (2018).
4. Bunin, G. Interaction patterns and diversity in assembled ecological communities. *arXiv preprint arXiv:1607.04734* (2016).
5. Allesina, S. & Tang, S. The stability–complexity relationship at age 40: a random matrix perspective. *Population Ecology* **57**, 63–75. ISSN: 1438-3896 (2015).
6. Grilli, J. *et al.* Feasibility and coexistence of large ecological communities. *Nature communications* **8**, 0. ISSN: 2041-1723 (2017).